DEVELOPMENT OF STRATEGY TO IMPROVE THE RECUPERATION OF REGENERATIVE BRAKING ENERGY FROM ELECTRIC TRAIN

CHONG KAH YUN

UNIVERSITI TUNKU ABDUL RAHMAN

DEVELOPMENT OF STRATEGY TO IMPROVE THE RECUPERATION OF REGENERATIVE BRAKING ENERGY FROM ELECTRIC TRAIN

CHONG KAH YUN

A project report submitted in partial fulfilment of the requirements for the award of Bachelor of Engineering (Honours) Electrical and Electronic Engineering

Lee Kong Chian Faculty of Engineering and Science
Universiti Tunku Abdul Rahman

April 2022

DECLARATION

I hereby declare that this project report is based on my original work except for citations and quotations which have been duly acknowledged. I also declare that it has not been previously and concurrently submitted for any other degree or award at UTAR or other institutions.

Signature   :

Name   : Chong Kah Yun

ID No.   : 1705699

Date   : 29/3/2022

APPROVAL FOR SUBMISSION

I certify that this project report entitled **DEVELOPMENT OF STRATEGY TO IMPROVE THE RECUPERATION OF REGENERATIVE BRAKING ENERGY FROM ELECTRIC TRAIN** was prepared by **CHONG KAH YUN** has met the required standard for submission in partial fulfilment of the requirements for the award of Bachelor of Engineering (Honours) Electrical And Electronic Engineering at Universiti Tunku Abdul Rahman.

Approved by,

Signature   :   *Chua Kein Huat*

Supervisor   :   Ir Dr. Chua Kein Huat

Date   :   22/4/2022

The copyright of this report belongs to the author under the terms of the copyright Act 1987 as qualified by Intellectual Property Policy of Universiti Tunku Abdul Rahman. Due acknowledgement shall always be made of the use of any material contained in, or derived from, this report.

ACKNOWLEDGEMENTS

ABSTRACT

Electrified rails with the recuperation of regenerative braking energy offer higher energy efficiency, lower carbon footprint, and lower operation costs than other systems without the recuperation of regenerative braking energy. However, unfavorable conditions such as inefficient recovery processes or system overload may arise due to improper energy handling. When these conditions occur, the regenerative braking energy needs to be dissipated via resistor banks to ensure system stability. This study investigates the amount of regenerative braking energy recovered under train operating conditions such as different station distances, train speeds, track elevations, and train's weight under different loading conditions. The recuperation rate of regenerative braking energy under different conditions is identified to prevent wastage of energy or overload. The rail power supply and distribution systems for Malaysia's MRT Line 2 are modeled using ETAP - eTraX software. The dynamic behavior of the trains has been included in the simulation model to improve the study's accuracy. The operating conditions with the highest amount of regenerative braking energy have been identified in this study. The simulation results show that by maintaining the ideal scenario of an optimum station distance of 0.9 km, the maximum efficiency of the regenerative braking system can be up to 60.10%. Maintaining the highest operation speed limits of 100 km/h, lowest elevation, and highest possible weight of the train, which is 253 tons with maximum passengers on board, the efficiency of recuperation of energy can be up to 51.70% for the regenerative braking system. An actual-world measurement is also being studied, and the outcome of the practical results are identical to the simulation outcome.

TABLE OF CONTENTS

LIST OF TABLES

LIST OF FIGURES

LIST OF SYMBOLS / ABBREVIATIONS

AARU	Automatic Assured Receptivity Unit
ESS	Energy storage system
MRT	MASS rapid transit
RTCR	Reversible thyristor-controlled rectifier
TCI	Thyristor line commutated inverter
AC	Alternating current
DC	Direct current
PS & DS	Power supply and distribution system
TPSS	Traction power substation
TERS	Traction Energy Recovery System
λ_w	Train Rotational Inertial

CHAPTER 1

INTRODUCTION

1.1　　　General Introduction

Transportation sector is considered one of the largest energy consumers, and it accounts for 25% of energy consumption globally (Khodaparastan, Mohamed and Brandauer, 2019a). Among all the transportation systems, electrified railways provide greater energy efficiency, a reduced carbon footprint, and lower operating and maintenance expenses than conventional diesel-powered trains (Mayrink et al., 2020). However, regardless of the existing benefits, enhancing the overall efficiency of the electric rail system is still critical as the population rises by each day. The need for train services will continue to rise, as will energy usage (Gao et al., 2019).

In railway study, there are four modes of operation for electric trains, namely accelerating, cruising, coasting, and braking. The braking mechanism of a railway vehicle is exceptionally complex but critical for traffic safety. A braking system is essential as it reduces vehicle speed by changing the kinetic energy to a different form (Günay, Korkmaz and Özmen, 2020a). Present-day electric rail transit appears to rely on regenerative braking to decelerate. The benefits of utilizing regenerative braking are that it can recover a portion of energy to the electrical network during the braking process, improving the energy efficiency of the overall system. Given that frequent stops are a significant characteristic of railway vehicles, braking energy recuperation offers excellent potential to reduce energy consumption in power rail systems (Hosseinipour and Zolghadri et al., 2019).

Generally, the produced energy from regenerative braking is the auxiliary supply for the train. However, the excess energy that is not being utilized may cause the system to be over-voltage. In order to maintain the system stability, the energy must dispose of through the resistor as heat energy. There are numerous approaches to managing regenerative braking energy in railway vehicles economically. The first solution is synchronizing the movement characteristics of the loads along the traction power supply lines, usually called "Timetable Optimization". Another option is to use a

reversible substation to revert the regenerative braking energy to the external grid. The third alternative is to store the energy generated by regenerative braking in an energy storage system (ESS).

A properly planned schedule can recover and reutilize a significant amount of regenerative braking energy. Several studies have been carried out to investigate the factors that affect the recuperation of regenerative braking energy. The regenerative braking system (RBS) performance is affected by numerous factors, including the structural design of the power-train system, the control strategy, and braking conditions on the operation stage (Bae et al., 2007; Lu et al., 2014; Dong et al., 2017).

The Malaysia Mass Rapid Transit 2 (MRT Line 2) system is modeled using ETAP software in this study. This project focuses on the effects of the train station distance, the maximum speed limit of the track, track elevation, and the train's weight under different loading conditions on the efficiency of recovery of regenerative braking energy. Thus, a solution that optimizes the highest amount of regenerative braking back to the system is investigated.

1.2   Importance of the Study

There are several solutions available that can utilize regenerative braking energy. However, the power flow exchange between the trains and the power distribution network is not always allowed. It depends on whether the catenary can store the energy that comes from the vehicles during the deceleration phase.

Energy recovery is also possible when adjacent trains accelerate in the same power supply section as the stopping one. However, the strategy is fraught with difficulty as the train's acceleration during the regenerative braking is never guaranteed. Furthermore, train headway and system age influence the amount of energy used by nearby trains (Popescu and Bitoleanu, 2019). Excess energy generated and unused may cause unnecessary wastage of energy and hazardous situation. Therefore, it is essential to understand the recovery process of regenerative braking energy to utilize it to maximum potential.

1.3   Problem Statement

The Malaysia MRT Line 2 project recuperates the regenerative braking energy by implementing the reversible substation, namely Traction Energy Recovery System (TERS). Even though the reversible substations are designed to effectively return regenerative braking energy to the upstream network, various factors are still needed to consider if maximum regenerative braking energy is targeted. Furthermore, the installation of TERS is not available for all the substations on the mainline. Due to this reason, there is a possible drawback when the substation with TERS is not available. For example, when the substation with TERS is under maintenance, the neighboring substations of the maintaining substation may not effectively recuperate the regenerative energy as the operating substation's distance is too far from the train's braking location.

To account for the limitation of the reversible substation, we need to assess and understand the traction energy that can absorb from the railway system under a different scenario so actions can be done to reduce wastage.

For the reason that the optimal siting management of stations and several dynamic properties of tracks and substations are also crucial in determining the system's efficiency in recuperating the energy available, this research will analyze and obtain the optimum strategy to recuperate the regenerative braking energy with an optimum scenario considering on the siting, speed, elevation and train's weight.

1.4   Aim and Objectives

This research aims to investigate the nature of regenerative braking in the railway system and develop a strategy to improve the recuperation of regenerative braking energy for electric rail transit. The objectives of this research are:

(i)   To investigate various challenges encountered by regenerative braking of electric trains.

(ii)   To develop a simulation model for regenerative braking of electric trains.

(iii) To evaluate the performance of the simulation model developed.

1.5   Scopes and Limitations of the Study

The scope of study in this project includes investigating on the effects of the train station distance, the maximum speed limit of the track, track elevation, and the weight of the train under different loading conditions on the efficiency of recovery of regenerative braking energy with the MRT Line 2 model.

Due to the simulation tools not being able to generate the necessary condition, the study does not include the regenerative braking energy that is recuperated during the synchronization of the loads along the traction power supply lines. Furthermore, the condition included various uncertainty that needed to be considered and may complicate the simulation. In addition, the noise and harmonic distortion which might be generated from the various practical situation will also be excluded from the study.

1.6   Contribution of the Study

This research has been accepted into the "2022 IEEE International Conference in Power Engineering Applications (ICPEA 2022)" conference regarding engineering field contribution. The 2022 IEEE International Conference in Power Engineering Applications (ICPEA 2022) is held from 7 March to 8 March 2022. The conference brings together academicians and other stakeholders and researchers, policymakers, and industry groups to present research expertise and discoveries on a variety of power engineering application subjects. The study was published under the title of "An Investigation on Recuperation of Regenerative Braking Energy in DC Railway Electrification System" by author Mr. Chong Kah Yun. The conference paper is being accepted on 11 January 2022, and it is being presented on 7 March 2022. Lastly, the paper is stamped for IEEE Xplore on 24 March 2022.

This study can be used for future research related to energy storage sizing or inverter siting and sizing references (Sang Hoo et al., n.d.). This project investigates the different aspects that affect regenerative braking energy's recuperation. Therefore, with the results, it can be observed that the system's electrical behavior is affected by different scenarios being installed

into the setup. The resulted scenario can be severe and substantial in some conditions. Therefore, the study can assist in the energy storage or inverter sizing activities as it assesses various resulting scenarios such as peak voltage in different system setups and tests. Furthermore, it can also assist in the siting activities of the system as it investigates the effect of distance on the recuperation process.

1.7   Outline of the Report

This project investigates the effects of the train station distance, the maximum speed limit of the track, track elevation, and the train's weight under different loading conditions on the recovery efficiency of regenerative braking energy. After investigating the different aspects affecting the recuperation, a strategy is proposed to optimize the maximum recovery rate of regenerative braking energy back to the system.

An in-depth study on the train dynamic and kinematics in energy recuperation is presented in Chapter 2. The MRT Line 2 railway electrification system is modeled and simulated in ETAP - eTraX software in Chapter 3. The chapter will contain the system models and descriptions of MRT Line 2, Malaysia. Chapter 4 evaluates the results of the variously modeled system and re-analyses the recuperation with an improved model, which incorporates all of the improving aspects into the system to determine how much energy may be recovered before and after.

CHAPTER 2

LITERATURE REVIEW

2.1 Introduction

This chapter summarizes previous literature relevant to the topic of study that has been conducted in recent years. This chapter aims to find a gap in the literature where a new contribution may be made and examine the various approaches employed in this field.

2.2 Train Kinematic in the Railway System

The kinetic energy of the rolling stock is used to overcome aerodynamic drag, the rolling resistance, and the braking system (Dong et al., 2017). A regenerative braking system recaptures part of the braking process's energy by converting the energy back to electrical energy, which minimizes the energy required to convert into unrecoverable heat energy with frictional brakes. The control strategy and braking condition become the regeneration energy's significant factors when maximum energy recuperation is desired during the braking process (Popescu and Bitoleanu, 2019). The control strategy usually involves a complex optimization strategy and scheduling. In contrast, the braking condition engages on dynamic factors such as the train's velocity and the gradient between the destination and the starting point (Tian et al., 2020).

Next, the force distribution strategy may indirectly affect the recoverable energy as the energy is dissipated in overcoming the resistance. Many factors need to be considered to prevent excessive energy loss to recuperate the energy effectively, such as the braking rate, the vehicle, rolling resistance and aerodynamic drag, track resistance, and the gradient factor of the rail (Bae et al., 2007; Lu et al., 2014; Dong et al., 2017; Tian et al., 2019).

2.2.1 Train Kinematic Formula Modelling

Railway kinematics modeling can be established using Lomonossoff's equations, as shown in Equation 2.1. The tractive effort, gradient, and vehicle resistance influence how the vehicle moves in the longitudinal direction. In

Lomonossoff's equation, the vehicle mass can be obtained by adding the tare and payload masses, as shown in Equation 2.2. The train's effective mass M_e, on the other hand, should include the train rotational inertial, λ_w, to the tare mass as shown in Equation 2.3. The rotational inertia effect is usually between 5% and 15% of the total rotational inertia (Lu et al., 2014; Tian et al., 2019).

$$M_e \frac{d^2 s}{dt^2} = F - Mgsin(\alpha) - R \qquad (2.1)$$

$$M = M_t - M_l \qquad (2.2)$$

$$M_e = M_t \times (1 + \lambda_w) + M_l \qquad (2.3)$$

where

M_e = effective mass, ton

F = tractive effort, N

M = vehicle mass, ton

R = rolling resistance, N/ton

g = gravitational acceleration, N/kg

α = slope angle

λ_w = train rotational inertial

2.2.2   Train Tractive Effort

Figure 2.1 shows the typical train's tractive effort curve, where adhesion and engine design limit the locomotive's maximum tractive effort against speed. The minimum point of contact between the wheel and the rail causes the adhesion limit. The maximum frictional force applied between this contact point is the maximum forward force that a wheel can apply to a rail before it slips (Polach, 2001; Grassie and Elkins, 2005; Lu et al., 2014).
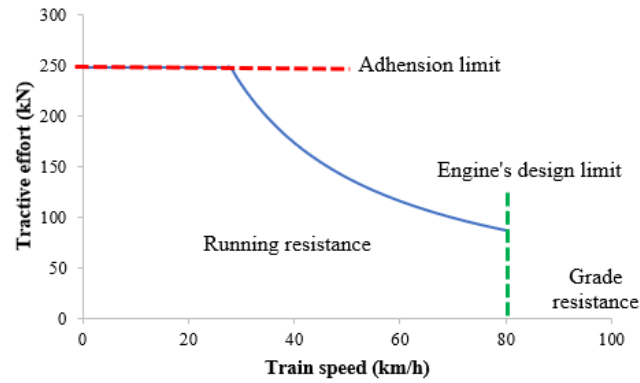
Figure 2.1: Train's tractive effort curve.

On the other hand, the engine design will result in velocity limitations. The tractive force depends on the power that a motor can supply. The engine power often refers to the rated power, a power output that the engine can sustain based on a specific testing technique. These are the fatigue limits for a locomotive to prevent disasters such as motor overheating and damage to the system (Grassie and Elkins, 2005).

2.2.3   Rolling Resistance and Track Grade Resistance

Rolling resistance and track grade resistance are two types of train resistance. The rolling resistance of a train is determined by its mass, shape, and aerodynamic characteristics, as described by the Davis Equation in Equation 2.4. Run-down experiments are commonly used to determine the Davis constant coefficients A, B, and C (Lu et al., 2014; Tian et al., 2019).

$$R = A + Bv + Cv^2 \tag{2.4}$$

where

R = rolling resistance, N/ton

v = velocity, m/s

Coefficient A is connected to axle load and is influenced by roller bearing and track resistance. On the other hand, coefficient B depends on flange friction or rail wave action elements, where the quality of the track and the train's stability are considered. Besides that, coefficient C represents the

aerodynamic resistance of the rolling stock during high-speed traveling (Lu et al., 2014). Apart from the rolling resistance, the train also experiences grade resistance that acts as a gravitational resistive force when the rolling stock goes uphill or downhill (Grassie and Elkins, 2005). The force from grade resistance shown in Equation 2.5 will be positive when going uphill and negative when going downhill.

$$F_g = Mgsin(\alpha) \tag{2.5}$$

where

F_g = gravitational force, N

The value of M can be obtained using the formula shown in Equation 2.2. In contrast, g are the gravitational acceleration and slope angle, respectively. The tractive effort curve, including the running resistance and grade resistance, is shown in Figure 2.2.
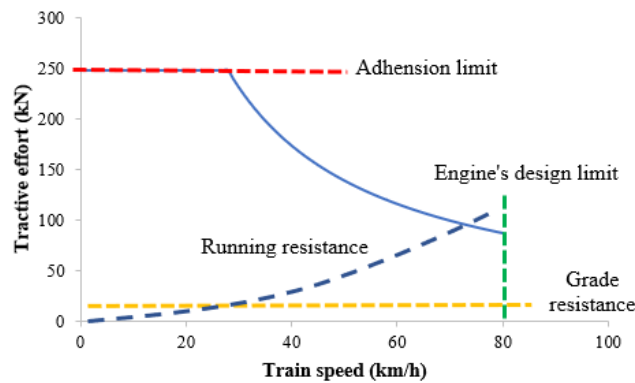
Figure 2.2: Practical train's tractive effort curve.

2.3   Braking System in Railway

The braking system is considered the most crucial function in railway vehicles. It converts all or part of the moving vehicle's kinetic energy into other energy to slow it down. If necessary, the vehicle's braking systems will bring it to a complete stop. It also aids in preventing weight-related stresses on gradients, allowing the vehicle to keep a consistent speed and maintain its

condition on an inclined track subjected to weather factors such as wind and rain (Straub and Jennison Knorr-Bremse, n.d.).

The railway system employs various braking technologies, all of which can be classed as adhesion or non-adhesion braking. However, adhesive-type brakes are the ones that are generally utilized in railway vehicles (Günay et al., 2020). Figure 2.3 shows the different types of braking utilized in the railway system.
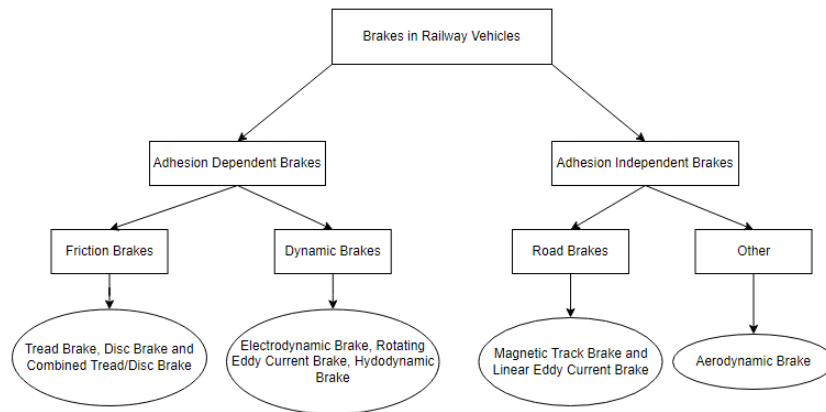
Figure 2.3: Different types of braking in the railway system (Günay, Korkmaz and Özmen, 2020a).

Most traction energy in a railway system is expended in braking actions. The amount of lost energy in the braking process may be up to half of the total energy delivered to the rolling stock depending on the category of power supply system used (Hosseinipour and Zolghadri et al., 2019). Due to friction brakes and various factors, approximately one-third of the braking energy during dynamic braking is not recovered. Figure 2.4 shows the traction energy flow diagram of the typical railway system.
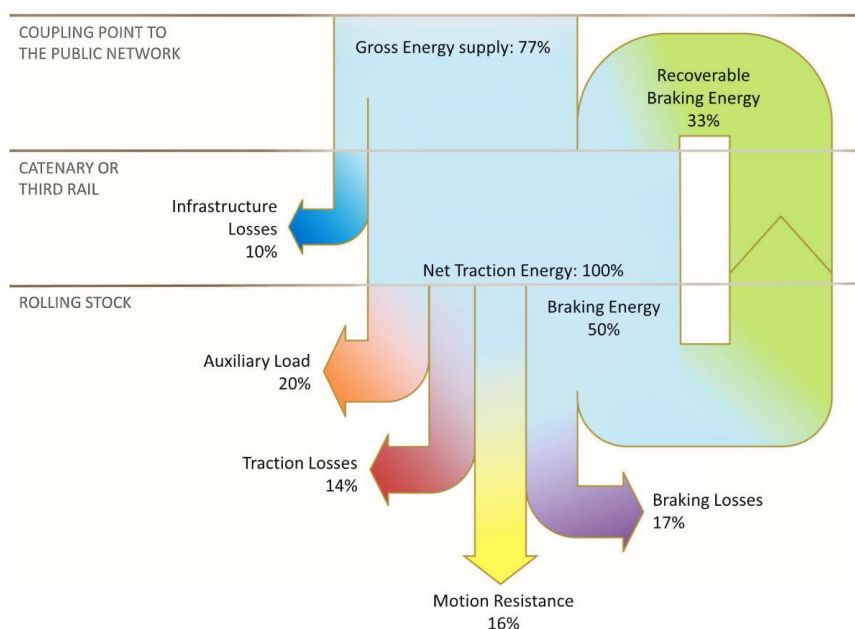
Figure 2.4: Traction energy-flow diagram (Tian et al., 2020).

For this reason, improving the design of a braking system is a significant practical challenge. Although various brakes are available, each approach contains its own set of limitations and constraints. The braking system should be considered thoroughly as different brake techniques are likely more suitable for specific usage. Likewise, the vacuum braking system in air and vacuum brake systems is not suitable for high-speed trains. On the other hand, air brakes can be more efficient than vacuum brakes but require a considerable distance (Günay et al., 2020).

2.3.1 Regenerative Braking

Regenerative braking is a type of electrodynamic braking technique. It utilizes the law of conservation of energy to decelerate the vehicles. When mechanical brakes are employed in a normal condition, the kinetic energy is wasted in the form of heat due to frictional force. However, in regenerative braking, the vehicle slows down by reversing the motor's function. The ability of electric motors to serve as generators is required to convert kinetic energy into electrical energy is known as dynamic braking (González-Gil, Palacin and Batty, 2013). A properly planned scheme can recover and reutilize a significant amount of regenerative braking energy.

However, the regenerative braking method has its downside in that the brake systems may occasionally fail due to intricate circuits. Suppose no powered rail transport can absorb such regenerated energy. In that case, it raises the voltage in the catenary line, resulting in an unstable system. Once it reaches a specific threshold, the regenerative energy will be consumed as heat in the railcar's resistor (Bae et al., 2007). Therefore, despite the several benefits of regenerative braking, it is rarely used for emergency braking. The poor utilization planning in the system may also cause the third rail or pantograph to surges in voltage and eventually happen to overvoltage. When this happens, regenerative braking operations will cease entirely, and the braking force may alternatively supply by a mechanical brake. Therefore, well-planned utilization schemes should come together when regenerative braking is being harnessed into the system. The scenario where the cutoff happens is shown in Figure 2.5.
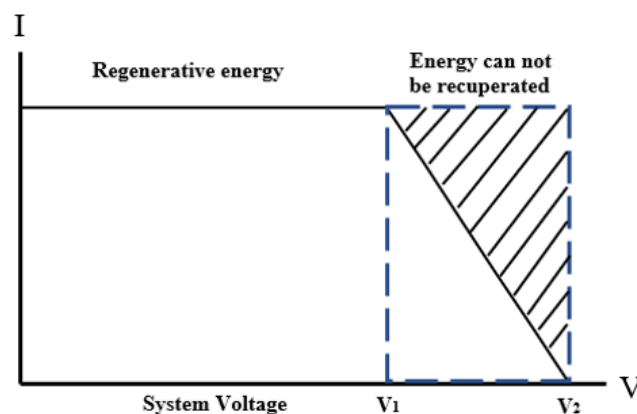
Figure 2.5: Cutoff voltage for recuperation of energy (Wang et al., 2014).

2.4　　The Effort to Improve the Recuperation of Energy

Various studies, attempts, and comparisons have increased regenerative energy recovery in the railway system. Regenerative braking energy can be recovered and repurposed in large amounts if the schedule is well arranged. Several studies have explored the parameters that influence regenerative braking energy recovery (Du et al., 2016; Khodaparastan et al., 2019).

2.4.1 Selection of Recuperation Methods

Choosing the recuperation method becomes crucial for improving the overall system's efficiency. Putting aside timetable optimization and considering only the energy storage system and reversible substation. Due to decreased transformation losses, recovery of braking energy via reversible substations may be deemed a somewhat more efficient solution. Other notable merits of reversible substations over ESS include requiring less space, having lesser safety constraints, and maintenance does not disrupt rail system operations. However, if a fine-tuned analysis for identifying excellent placements is not made, the resistive losses may be relatively substantial. Furthermore, the investment may be relatively costly (Fazel, Firouzian and Shandiz, 2014).

2.4.2 Optimal Siting and Sizing

The best energy capacity and locations for storage devices have long been a popular research topic in electrical engineering. The consideration for optimal siting and sizing is to improve the overall efficiency of the systems while minimizing the costs incurred in the system (González-Gil, Palacin and Batty, 2013).

The primary goal of many studies is to find the optimal scale of energy storage systems and possibly minimize the overall operational and investment costs. Electrical railway systems' energy storage sizing problem is still an emerging research field for stationary energy storage. It has been asserted that oversizing the ESS will unnecessarily increase the system's weight and volume. At the same time, under-sizing may result in significant energy waste (Wu et al., 2020).

When the ESS is used in the railway system, allocating the storage device onboard will accumulate more train mass and necessitates more room for their accommodation. As a result, stationary ESS installed within the substations is typically favored for railway systems (Xia et al., 2015). However, selecting an optimal location is a complicated process. It is the most significant element in planning a storage device or distribution system. Determining the optimal location to install an ESS to meet electrical power demands is critical, as it can significantly impact power quality, future operating costs, and investment costs.

Through appropriate location and size optimization, financial savings of up to 5.84% can be realized and the energy consumption saving can reach up to 9% (Wu et al., 2020). Aside from ESS, studies also found that a significant amount of energy can be restored by choosing a proper location for inverters and achieving energy savings (Hosseinipour and Zolghadri et al., 2019).

2.5 Summary

This chapter describes the basic operation of the train kinematics and previous efforts from different studies. Besides, various types of railway braking systems are also being discussed. There is limited study that specifically investigates the impact of station distance, the train's speed, the elevation of the train station, and the train's weight on the recuperation of energy in the railway electrification system.

CHAPTER 3

METHODOLOGY AND WORK PLAN

3.1   Introduction

This chapter discusses the methods being utilized to improve the recuperation of regenerative energy in the railway electrification system. This section will provide a brief system description of Malaysia's MRT Line 2 mainline characteristics. Modeling in ETAP software will be done based on these parameters provided.

After that, several scenarios with a different methods of handling regenerative energy will be implemented to investigate the impact of regenerative braking recuperation.

3.2   System Description of MRT Line 2 Malaysia

3.2.1   Power supply and distribution system

The MRT Line 2 is Malaysia's, officially known as the Sungai Buloh-Serdang-Putrajaya Line. It is the second MRT line to be developed, with a proposed length of 52.2 km, 13.5 km underground. A total of 36 stations will be built, 11 of which will be underground. Figure 3.1 shows the route of MRT Line 2.
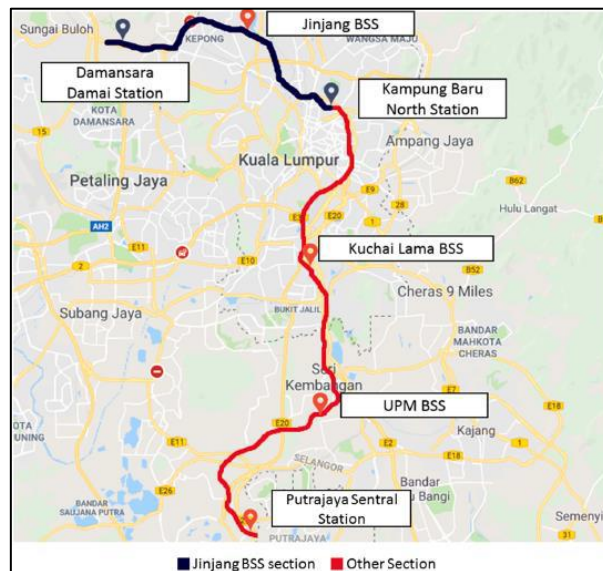
Figure 3.1: Overview of SSP line alignment.

The Power Supply and Distribution System (PS &DS) for the whole MRT Line 2 consists of the following:

- Three 132/33kV, 2x40MVA bulk supply substations (BSS)
- Twenty-two 33kV/750V DC, Traction Substations (Elevated Section)
- Six 33kV/750V DC Traction Substations (Underground Section)
- Three 33kV/400V, 2x1.25MVA Intervention Shaft Substation
- One 33kV/400V, 2x2MVA Ventilation Shaft Substation.
- Depot Section: Two 33kV/750V, 2x3.5MVA Rectifier transformers.
- Twenty-one 33kV/400V, 2x1MVA to 5MVA Utility buildings

In MRT Line 2, there are twenty-eight substations, each with two rectifier transformers and two auxiliary transformers. Rectifier transformers are to supply the DC traction loads. All the substations are supplied with two 33kV circuits to maintain redundancy.

3.2.2 Traction power system parameters

Only a section of MRT Line 2 will be included in the simulation in this project. The specification of the traction characteristic is summarized in Tables 3.1, 3.2, and 3.3.

Table 3.1: System parameters.

Description	Values
Nominal voltage	750 V_{dc}
Inverter triggering voltage	830 V_{dc}
Maximum system voltage (including under regenerative braking conditions)	900 V_{dc}
Rated continuous direct current	2667A for 2MW TPSS
Internal Resistance of Rectifier and Inverter	100m-ohm (assumption)

Table 3.2: Rectifier Parameters.

Description	Values / Information

AC Rating	
Rated Power	2125.8 kVA
Rated Voltage	0.585 kV
Rated full load ampere	2098 A
Rated %PF	96 %
DC Rating	
Rated Power	2000 kW
Rated DC Voltage	750
Rated full load ampere	2667 A
Imax%	150 %

Table 3.3: 3-Winding Transformer Parameters.

Description	Values / Information
Type	Liquid-Fill
Class	ONAN/ONAF
Rating (Voltage, VA, FLA)	Prim: 33kV, 2.3 MVA, 40.24A Sec: 0.585kV, 1.15 MVA, 1135A Ter: 0.585kV, 1.15 MVA, 1135A
Impedance: Positive (%Z, X/R)	PS: 6, 10 PT: 6, 10 ST: 12, 10
Impedance: Zero (%Z, X/R)	PS: 80, 10 PT: 80, 10 ST: 80, 10

3.2.3 Cable Resistance

The DC cable used for the feeder or return cable is 500mm^2 Cu. The cable resistance is assumed to be 0.0391 Ω/km, and the running rail's resistor is 22 Ω/km. The resistance increase due to the temperature factor will be ignored for the case study.

3.2.4 Rolling Stock Characteristic

The general dynamic performance with rolling stock utilized in MRT 2 is stated below. The simulation should stick with the characteristic below. The number of axles of the rolling stock is two motor cars at the front and back

and two trailer cars in the middle with a total length of 90m. The rolling stock's area is 11.0408 m^2, following the factual data provided by the project developer. Table 3.4 shows the information on the rolling stock mentioned above and its electrical characteristics.

Table 3.4: Rolling stock characteristic.

Train configuration	4 cars (M-T-T-M) M: Motor car, T: Trailer Car
The total length of the train	90m
Total weight	218 ton
Maximum operating speed	100 km/h
Maximum voltage in the traction	900 V$_{dc}$
Minimum voltage in the traction	500V$_{dc}$
Minimum speed for regenerative braking	5 km/h
Maximum voltage for regenerative braking	950 V$_{dc}$
Minimum voltage for regenerative braking	500 V$_{dc}$
Auxiliary power per car	236.48 kW / train
Coasting operation	Not applicable
Starting resistance of the train	49N / ton

Figure 3.2 shows the tractive effort curve of the train utilized in the model. The peak tractive effort for the rolling stock is 248 kN when the speed is between 0 km/h to 29 km/h. The tractive effort curve decreases when the speed reaches 29 km/h. The braking effort curve set for the rolling stock is shown in Figure 3.3. The peak braking effort for the rolling stock is 182 kN when the speed is between 6 km/h to 60 km/h.
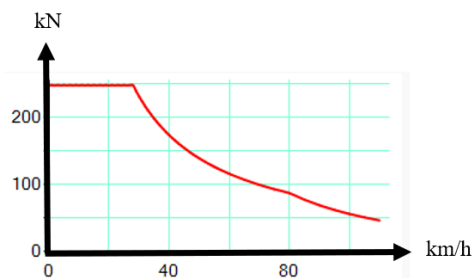
Figure 3.2: Tractive effort curve.
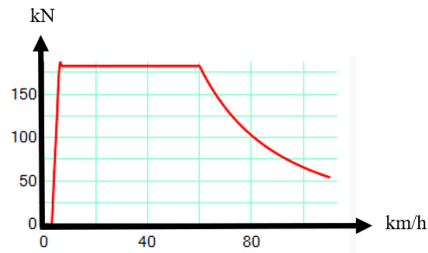
Figure 3.3: Braking effort curve.

3.2.5 Inverter Rating

MRT Line 2 involves several Traction Energy Recovery System (TERS) units. Each TERS consists of an inverter and an inverter transformer. TERS allows the excess power on the power rail from regenerative braking to be transferred back to the 33 kV distribution grid.

The generated voltage from the TERS must be within the TNB Supply Handbook limit of 33kV system, which is 33kV ±5% during normal and 33kV ±10% during contingency conditions. Besides that, the TERS should be shielded from all surges, harmonics, and over-voltages in terms of safety management. Table 3.5 shows the operating system rating of the TERS.

Table 3.5: TERS specification.

Description	Values
Power rating	550 kW
Input voltage	$820 \text{ V}_{dc} - 1000 \text{V}_{dc}$
Output voltage	800 V_{ac}
Maximum instantaneous power	3009 kW

3.3 ETAP Modelling of MRT Line 2 Power System

3.3.1 Bulk system substation

The MRT Line 2 system is being modeled in ETAP - eTraX software. Tenaga Nasional Berhad (TNB) supplies the entire power requirement of the SSP line. The traction power is then distributed among three bulk supply substations. The traction power substations will obtain power from the BSS and supplies it to the other systems through the third rail at 750 V.

Figure 3.4 shows the bulk substation (BSS), which comprises a transformer rated at 50 MVA that steps down the voltage from 132 kV to 33 kV to feed to the TPSS and a 160 kVA auxiliary transformer that will further step down the voltage from 33 kV to 0.4 kV for auxiliary purposes.
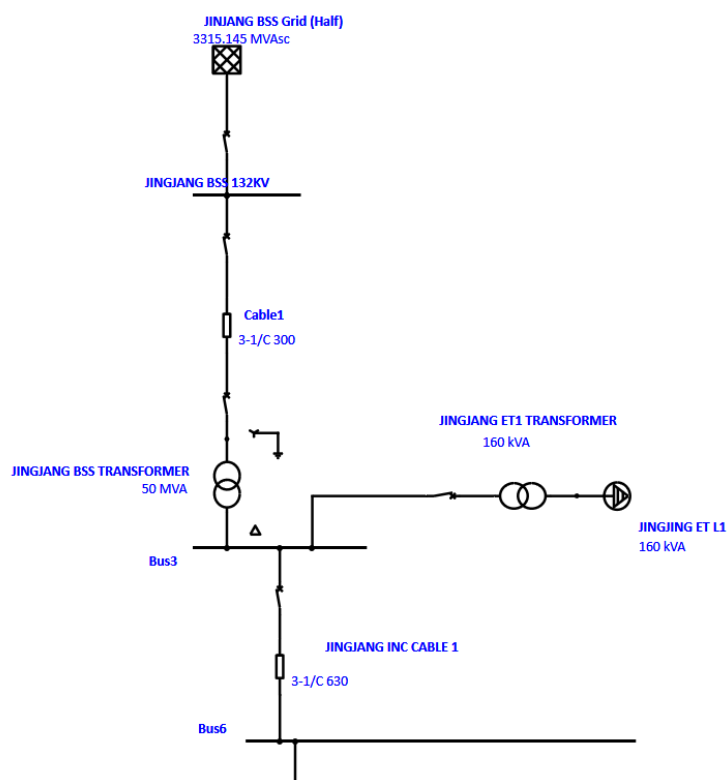
Figure 3.4: Bulk system substation.

3.3.2 Traction Power Substation in MRT Line 2 DC Rail System

Figure 3.5 then shows the schematic of MRT Line 2's DC electric rail transit system. The electric rail transit system is supplied by one traction power substation (TPSS) positioned along the railway line. The TPSS consists of 2 rectifier transformers rated at 2.3 MVA for the primary side and 1.15 MVA for the secondary and tertiary sides, which step down and rectifier the AC voltage to 750V DC voltage. Furthermore, the TPSS also consists of 2 auxiliary transformers for the utility buildings' auxiliary purposes.

Figure 3.6 shows the train platform and station model used in this project. The system consists of northbound and southbound, which will receive the power from the rectifier transformer to energize the trains. The MRT Line 2 system consists of elevated stations and underground stations.

Therefore, the rolling resistance for the open-air and tunnel environments will differ. The rolling resistance of the tunnel scenario is given in equation (6). The system is modeled based on the R_t provided by the project developer, where bearing resistance is 0.012932123 (kN/ton), rolling resistance is 0.00014764405 (kN/ton) *(hr/km), and air resistance of 2.09424E-07 (kN/ton) *((hr/km)^2).
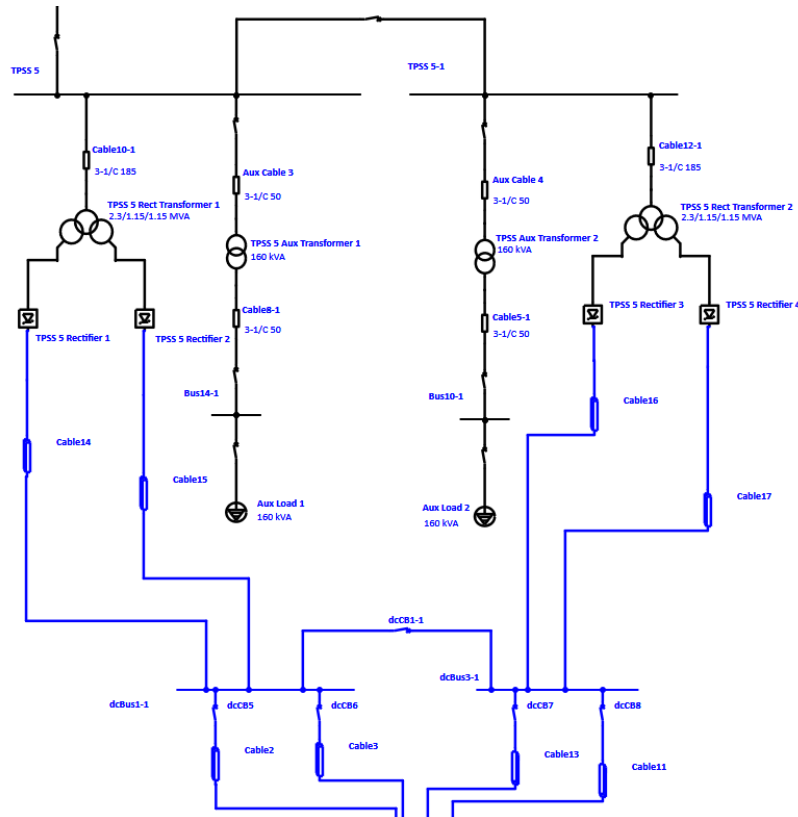
Figure 3.5: Traction power substation of MRT Line 2.
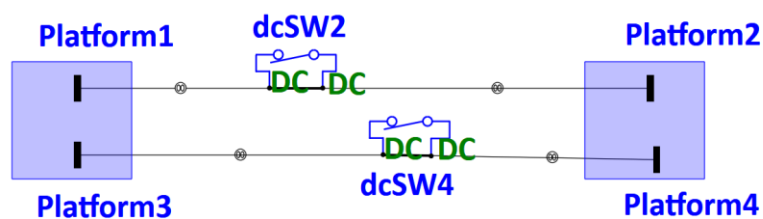
Figure 3.6: Stations and track modeling in EtraX.

3.3.3 MRT Line 2 Section Modelling

The modeling of the project will include only the section of MRT Line 2 for case study purposes, which includes two passenger stations and traction power substations (TPSS).

The simulation tool is eTraX^{TM}, which provides the most precise and adaptable software tools for assessing low to medium AC and DC voltage in rail power systems. It also included a train performance estimation that enabled the study and analysis of the impact of regenerative braking. Figure 3.7 shows the completed simulation model with MRT 2 system electrical characteristics.
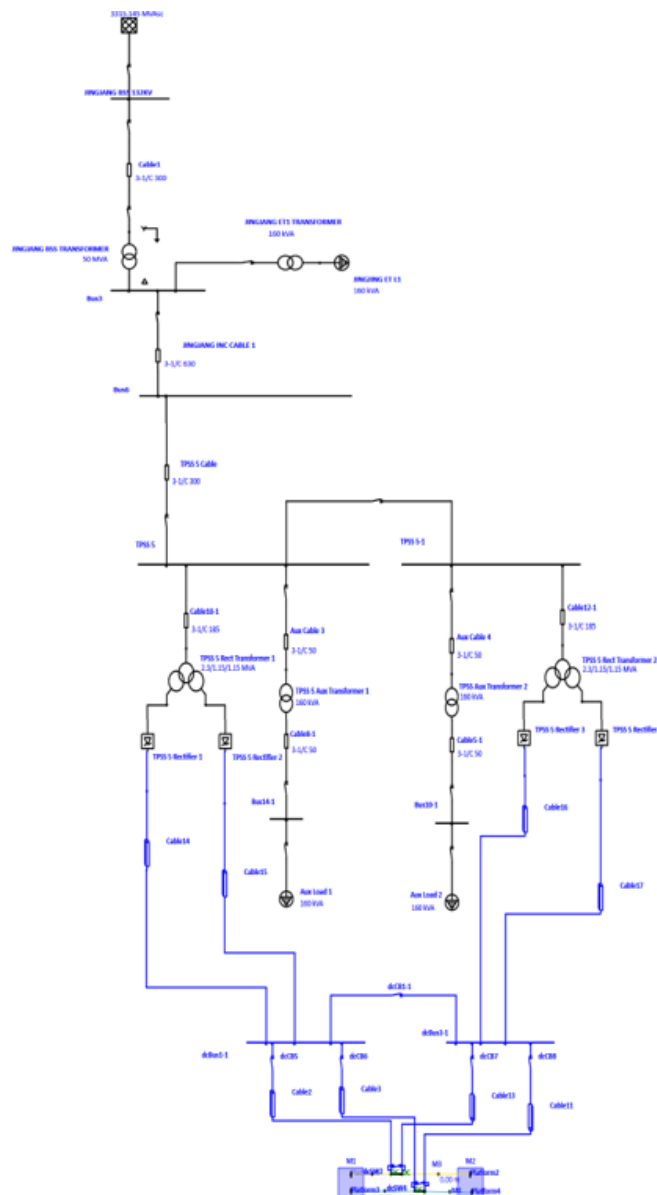
Figure 3.7: MRT Line 2 Model in ETAP.

3.4 Case studies with the EtraX Simulation Model

3.4.1 Initial Condition and Study Cases

Before the study case, the initial condition is set in the model as the pivot of the test. The station distance is initially set to 2.2km, and the speed limit is set to 110 km/h, the train's maximum speed. The elevation is not included in the initial condition, and the train loading condition is set at 218 tons. Table 3.6 below indicates the initial setup condition for the project's model.

Table 3.6: Initial condition of the study.

System Description	Settings
Northbound distance (m)	2231
Southbound distance (m)	2224
Maximum acceleration / deceleration (m/s²)	1
Dwell time (s)	40
Headway time (s)	109
Train's weight (tons)	218
Maximum Speed limit (km/h)	110
Station elevation (m)	0

3.4.1.1 Case study 1: Effect of Different Stations Distance

Case 1 studies the effect of different stations' distances on the recuperation of regenerative braking energy. In this case study, the track distance parameters are adjusted from 2.2km to 1.5km and 0.9km, indicating the longest, medium, and shortest distance. The values are chosen based on the MRT Line 2 maximum and minimum track distance between 2 stations. The medium distance is chosen based on the average distance of all tracks. Table 3.7 shows the parameters of case study 1 in EtraX.

Table 3.7: Parameters of case study 1.

System Description	Settings
Northbound distance (m)	**1500, 900**
Southbound distance (m)	**1500, 900**
Maximum acceleration / deceleration (m/s²)	1
Dwell time (s)	40
Headway time (s)	109

Train's weight (tons)	218
Maximum Speed limit (km/h)	110
Station elevation (m)	0

3.4.1.2 Case study 2: Effect of Different Speed Limits

In case study 2, the track distance is fixed at 2.2 km, while the track's maximum speed is set at 100 km/h, 83 km/h, 78 km/h, and 60 km/h. The speed of 100 km/h is the maximum train operation speed, while the 82 km/h and 78 km/h are the two average speeds of the MRT Line 2. The 60 km/h is the safe braking speed for the train to enter the platforms. Table 3.8 shows the parameters of case study 2 in EtraX.

Table 3.8: Parameters of case study 2.

System Description	Settings
Northbound distance (m)	2231
Southbound distance (m)	2224
Maximum acceleration / deceleration (m/s^2)	1
Dwell time (s)	40
Headway time (s)	109
Train's weight (tons)	218
Maximum Speed limit (km/h)	**100, 82, 78, 60**
Station elevation (m)	0

3.4.1.3 Case study 3: Effect of Different Station Elevation

In case study 3, the distance is fixed at 2.2 km, and different stations and speeds are set back to 110 km/h with elevations. The elevation between stations is set to 0.5 m, 3.7 m, and 18.3 m which are the minimum, medium, and maximum elevations. Table 3.9 shows the parameters of case study 3 in EtraX.

Table 3.9: Parameters of case study 3.

System Description	Settings
Northbound distance (m)	2231
Southbound distance (m)	2224
Maximum acceleration / deceleration (m/s^2)	1

Dwell time (s)	40
Headway time (s)	109
Train's weight (tons)	218
Maximum Speed limit (km/h)	110
Station elevation (m)	**0.5, 3.7, 18.3**

3.4.1.4 Case study 4: Effect of Different Train Weight

In case study 4, the train's weight is set at 152 tons, 218 tons, and 253 tons according to the loading data provided by the developer with the indication of AW0, AW3P, and AW5, respectively. Table 3.10 shows the parameters of case study 4 in EtraX.

Table 3.10: Parameters of case study 4.

System Description	Settings
Northbound distance (m)	2231
Southbound distance (m)	2224
Maximum acceleration / deceleration (m/s^2)	1
Dwell time (s)	40
Headway time (s)	109
Train's weight (tons)	**152, 253**
Maximum Speed limit (km/h)	110
Station elevation (m)	0

3.4.2 Simulation Procedure

The simulation procedure for all the case studies is the same. The TPSS should be replaced before carrying out the testing procedure for the analysis. Figure 3.8 and Figure 3.9 show the train's initial and final conditions during tests.
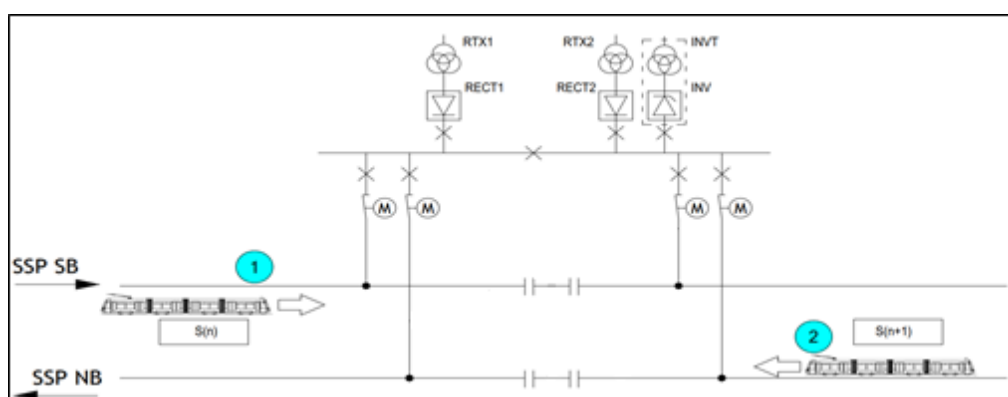
Figure 3.8: Testing initial condition.
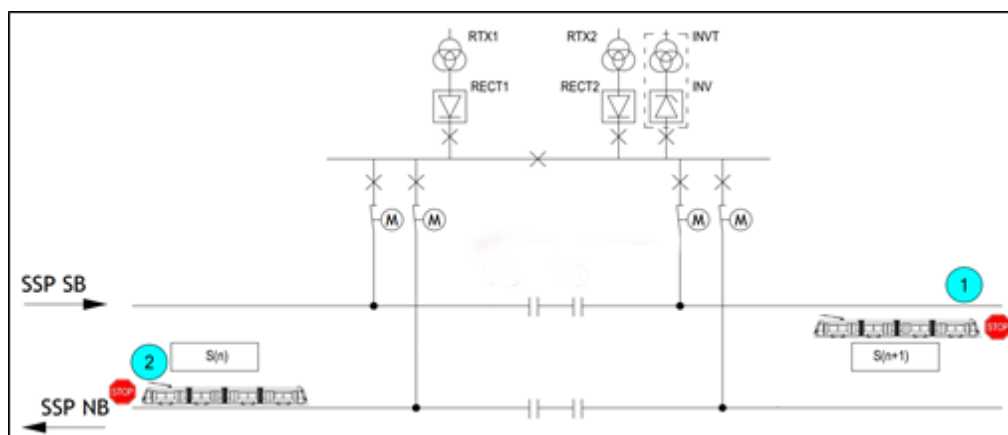
Figure 3.9: Testing final condition.

1. Before testing, we should ensure that the two trains are available at two passenger stations.
2. One train is located at SB station (Sn) and one at NB station (Sn+1). Refer to Figure 3.8 for each starting point.
3. Start moving both the trains at the same time.
4. Move the train from the station until it reaches to adjacent station and brake, as shown in Figure 3.9.
5. Record the regenerative braking energy from the braking process.
6. Repeat the procedure 1 to 5 with different parameters changes based on the initial condition set.

After completing the test, the condition where the recuperation rate of energy is at the peak will be used to establish a new model to compare with the initial condition and observe the rate of increment in energy-saving rate.

3.5 Practical Testing Data

3.5.1 Interface Test Procedure and Report for Load Test at Mainline Phase 1

The MRT Line 2 test information from the project procedure "INTERFACE TEST PROCEDURE FOR LOAD TEST AT MAINLINE PHASE 1" issued

on 18 September 2020 is being used as a reference for the research to generate a hypothesis for the studies. Competent engineers from CRSE Sdn Bhd have carried out the test procedure, and the report was issued on 20 November 2020.

3.5.2 Interface Test Scenario

Based on this procedure, the information for two test scenarios has been taken as a reference for the studies. The first test scenario includes the test between the station of Damansara Damai Station and Sri Damansara West Station of MRT Line 2. The second test scenario is located at the Kepong Baru Station and Jingjang Station of MRT Line 2. Table 3.11 and Table 3.12 shows some of the basic informations related to the test scenario.

Table 3.11: Description of the first test scenario.

System Description	Settings
Number of trains locate at Damansara Damai Station	1
Number of trains locate at Sri Damansara West Station	1
Distance of two stations (m)	1761
Maximum acceleration / deceleration (m/s^2)	1
Dwell time (s)	40
Headway time (s)	109
Train's weight (tons)	41.93 – 50.38
Maximum Speed limit (km/h)	40
Station elevation (m)	11.252

Table 3.12: Description of the second test scenario.

System Description	Settings
Number of trains locate at Kepong Baru Station	1
Number of trains locate at Jingjang Station	1
Distance of two stations (m)	928
Maximum acceleration / deceleration (m/s^2)	1
Dwell time (s)	40
Headway time (s)	109
Train's weight (tons)	52.05 – 55.32
Maximum Speed limit (km/h)	60

Station elevation (m)	1.464

The first test scenario has a geographical condition consisting of longer station distance and higher elevation between stations. Besides, the train is set at the weight of AW0, which is meant by empty passenger train weight. The test's vehicle can only accelerate up to 40 km/h for the travel.

The second test scenario taken has a geographical condition of short station distance with a low elevation between stations. The train consists of sandbags, indicating half-loaded passenger train weight. The train in the second test scenario is allowed to accelerate up to 60km/h.

3.5.3   Interface Test Procedure

In this test, the interface test activities start after the energization of all 750V DC systems of Mainline Phase 1 led by the power supply and distribution system company. The test of trainloads at the designed speed is to check that the protection systems are functioning as per the specified design.

The test procedure is similar to the procedure mentioned in section 3.4.2. Two trains will be initially placed at stations one and two. After being instructed to initiate the test, both trains will interchange the station, and the electrical system information will be retrieved afterward.

3.5.4   Outcome of the Interface Test Procedure

The test was being conducted in October 2020, and the tests were finished and concluded in the same month. The results from the system are extracted from the switchgear at the substations. The information from HSCB-00006, the inverters located in the traction power substation near the Sri Damansara Station and Kepong Baru Station is being studied. Figure 3.10 and Figure 3.11 show the feeder voltage and current feeder information extracted from the switchgear. The power is calculated using the information provided and shown in Figure 3.12 and Figure 3.13.
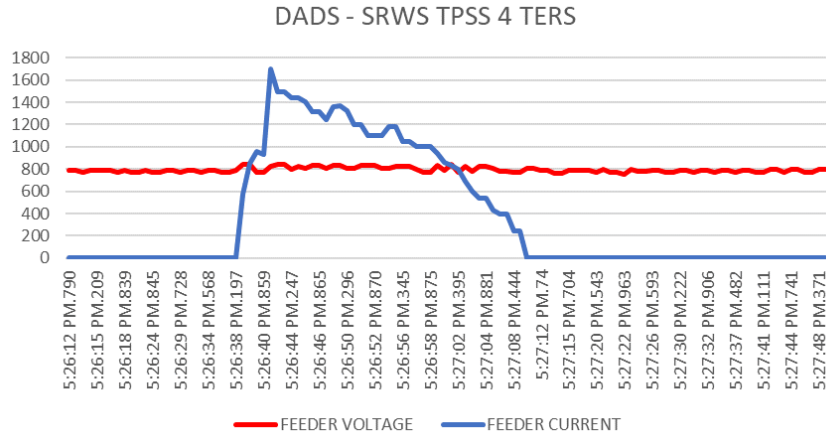
Figure 3.10: Results extracted from switchgear at TPSS nearby.
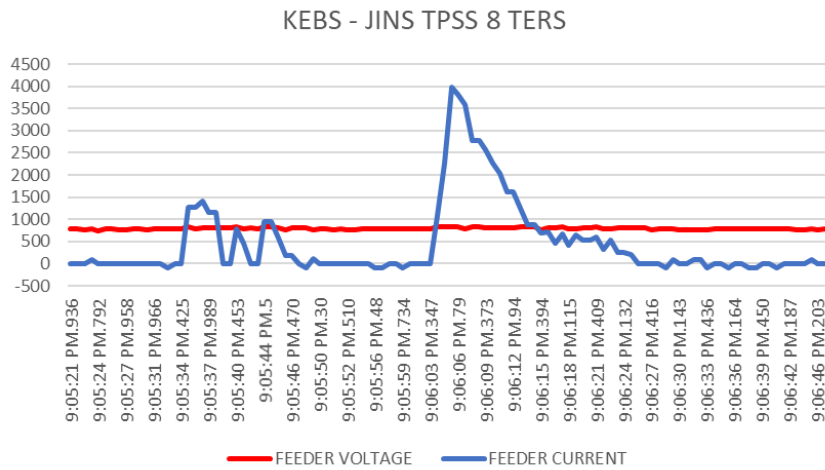
Figure 3.11: Results extracted from switchgear at TPSS nearby.
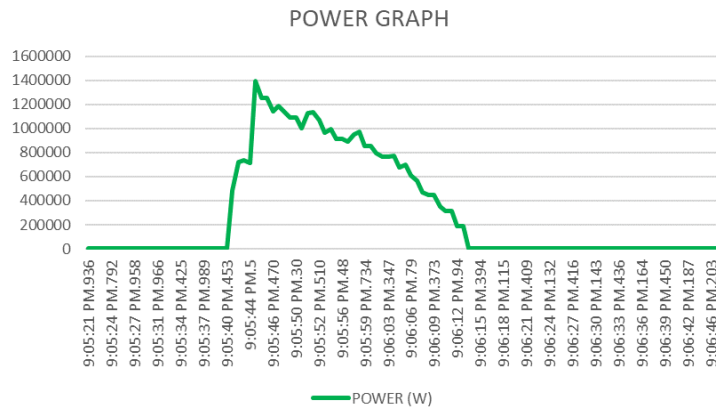
Figure 3.12: Power graph based on the results extracted at the first test.
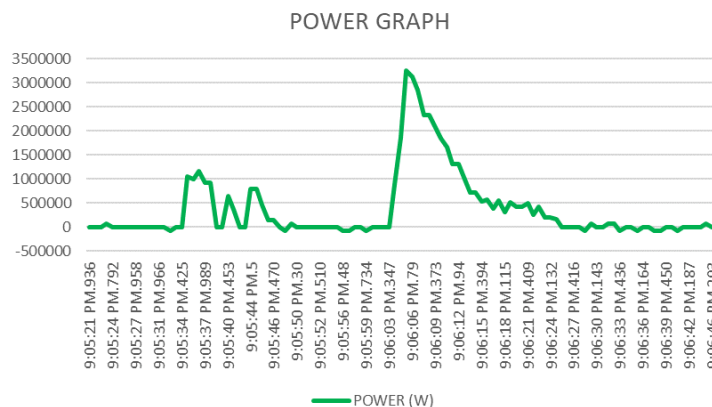
Figure 3.13: Power graph based on the results extracted at the second test.

Based on the results from the regenerative braking system in MRT Line 2, by calculating the area under the two power graphs, the energy recovered from the second test scenario is higher than the energy recuperated from the first test scenario. The energy recuperated for the first scenario is approximately around 9.23 kWh, while the second scenario recuperates around 11.3 kWh. The recuperation efficiency can be increased when the track has an optimum track distance, higher speed limitation, lower elevation, and high weight. However, the results can only be used to establish a general hypothesis due to limited information. Therefore, simulation in ETAP is done to get accurate results for the research.

3.6   Summary

This chapter provides the general specification of MRT Line 2, Malaysia, and a simulation model is being developed for various test purposes.

An MRT Line 2 model with an inverter characteristic is established to investigate the regenerative braking energy's recuperation. Different scenarios are investigated to precisely observe the recuperation rate in this study. Besides, real-world measurement and study based on the MRT Line 2 are also done in this section.

CHAPTER 4

RESULTS AND DISCUSSION

4.1 Introduction

In this chapter, the project's outcomes regarding the MRT Line 2 model and the performance of the regenerative braking system under different conditions will be discussed.

4.2 Calculation Method for the Efficiency of the Regenerative Braking System

The efficiency of the regenerative braking system which utilized the TERS can be calculated using Equation 4.1.

$$Rate\ of\ recuperation = \frac{E_{Final,no\ RBS} - E_{Final,RBS}}{E_{Final,no\ RBS}} \times 100\% \quad (4.1)$$

where

$E_{Final,\ no\ RBS}$ = Final energy consumption without RBE, kWh

$E_{Final,\ RBS}$ = Final energy consumption with RBE, kWh

The recuperation rate indicates the percentage of kinetic energy that can be converted back to electrical energy using the regenerative braking system. The higher the rate of recuperation percentage, the more energy can be recovered back, therefore indicating a higher efficiency of the system.

4.3 Effect of Different Stations Distance

Figures 4.1 and 4.2 show the train's energy consumption for the cases with- and without regenerative braking. The graph consists of different energy consumed by the longest distance track, medium distance track, and short distance track in MRT Line 2. The energy consumptions for the train without regenerative braking for the distance of 0.9 km, 1.5 km, and 2.2 km are 42.48 kWh, 33.28 kWh, and 23.84 kWh, respectively. Besides, the energy consumptions for the train with regenerative braking for the distance of 0.9

km, 1.5 km, and 2.2 km are 19.79 kWh, 14.30 kWh, and 9.51 kWh, respectively. Table 4.1 summarize the energy consumption taken during each test run in case 1.
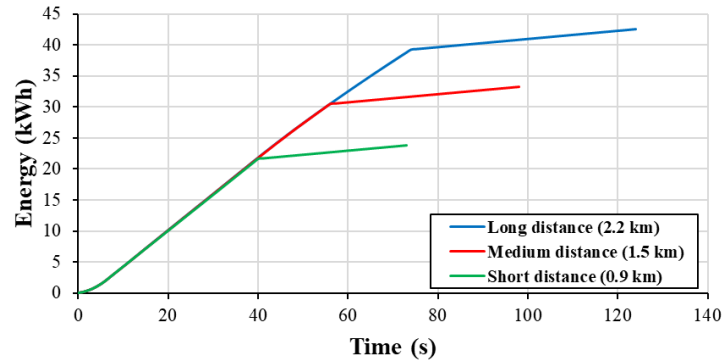
Figure 4.1: Power consumption of train at different distances without regenerative braking energy.
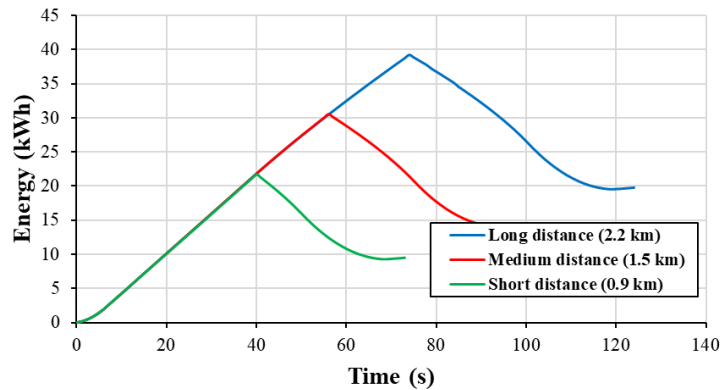
Figure 4.2: Power consumption of train at different distances with regenerative braking energy.

Table 4.1:   Case 1 results.

Distance (km)	Peak Energy Consumption with RBE (kWh)	Final Energy Consumption without RBE (kWh)	Final Energy Consumption with RBE (kWh)	Rate of Recuperation
2.2	39.19	42.48	19.79	53.41%
1.5	30.52	33.28	14.30	57.03%
0.9	21.68	23.84	9.51	60.10%

The maximum achievable speed for the scheduled trip is 103.8 km/h, 94.71 km/h, and 82.4 km/h for the track distance 2.2 km, 1.5 km, and 0.9 km,

respectively. The track with the maximum energy consumption is the longest track distance, consuming 42.5 kWh. The lowest energy consumption is the lowest track distance traveled which is 23.8 kWh. The medium distance, which is the average distance of all the station distances for MRT Line 2, consumes 33.3 kWh.

With the application of regenerative braking, the energy consumption is reduced by 53.41%, 57.04%, and 60.12% for the longest, medium, and shortest distances, respectively. During train operation, the speed of the moving train can be limited by the travel distance between the train as the vehicle's standard acceleration and deceleration is capped at 1 m/s^2. Therefore, with the same dwell time and headway time, the higher the station distance, the higher the energy consumption despite the system being with- or without regenerative braking. However, the shorter distances can cause a significantly higher regenerating braking energy recovered during the braking phase.

4.4   Effect of Different Speed Limits

Figures 4.3 and 4.4 show the train's energy consumption with- and without regenerative braking. The graphs below consist of the energy consumption for the highest speed, average speeds, and safety speed limit results. The energy consumption for the train without regenerative braking for the speed of 100 km/h, 83.16 km/h, 78.09 km/h, and 60 km/h are 40.37 kWh, 32.65 kWh, 30.57 kWh, and 24.52 kWh, respectively. Besides, the energy consumption for the train with regenerative braking for the speed of 100 km/h, 83.16 km/h, 78.09 km/h, and 60 km/h are 19.50 kWh, 17.97 kWh, 17.79 kWh, and 17.17 kWh, respectively. Table 4.2 summarize the energy consumption taken during each test run in case 2.
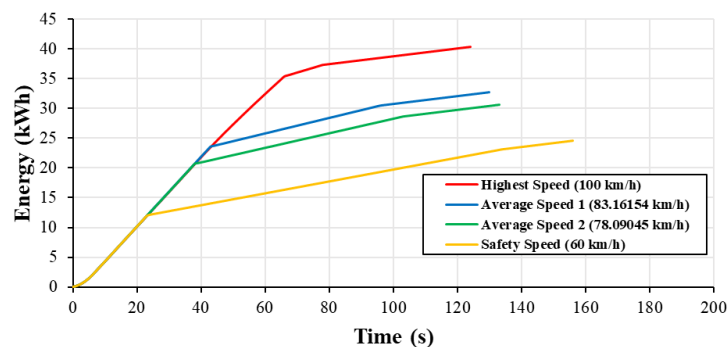
Figure 4.3: Power consumption of train at different speeds without regenerative braking system.
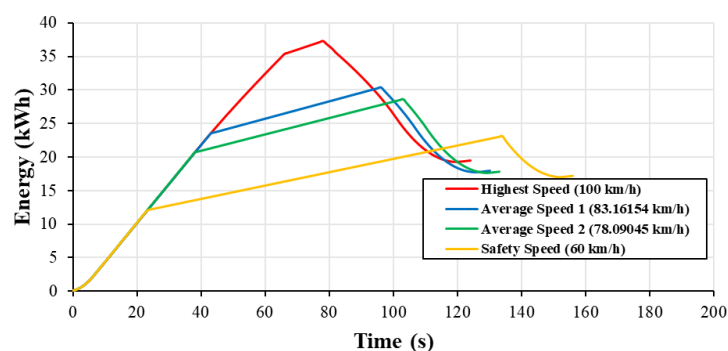
Figure 4.4: Power consumption of train at different speeds with regenerative braking system.

Table 4.2:   Case 2 results.

Speed (km/h)	Peak Energy Consumption with RBE (kWh)	Final Energy Consumption without RBE (kWh)	Final Energy Consumption with RBE (kWh)	Rate of Recuperation
100	37.34	40.37	19.50	51.70%
94.7	30.42	32.65	17.97	44.96%
82.4	28.60	30.57	17.79	41.81%
60	23.08	24.52	17.17	29.98%

From Figure 4.3, when the train moves at the maximum speed of 100 km/h, the train consumes 40.4 kWh of energy, and the accumulated energy consumption decreases as the maximum speed decreases. When the target operating speed is reduced, the total power required for the operation gradually decreases, reducing the total energy consumption. The highest energy can be saved by keeping the train moving at the slowest possible

speed. However, from Figure 4.4, when regenerative braking is utilized, the differences in energy consumption at different speed limits are significantly minimized, with the greatest speed consuming 19.5 kWh at 100 km/h only.

From Table 4.2, it can be observed that when the speed limit is reduced to 60 km/h, the rate of recuperation is significantly reduced. In contrast, the maximum speed limit of 100 km/h allows 51.70% of energy to be recuperated. Therefore, with a higher speed limit, the rate of recuperation of regenerative braking energy will be higher.

When regenerative braking is utilized, the speed of the operation does not contribute significantly to the total energy consumption. The higher the speed, the greater the presence of reverse braking power, resulting in more energy being recovered during the braking phase, compensating for the high energy expended. Therefore, as shown in Figure 4.4, the accumulated energy consumptions for all the speed limits are about the same as the case with the regenerative braking system. The only element influenced by the change in speed is peak energy. When the speed increases to 100 km/h, the peak energy is 37.3 kWh, whereas 60 km/h has peak energy of 23.1 kWh. There is a 38.2% difference in peak energy when the maximum operating speed increases from 60 km/h to 100 km/h.

4.5   Effect of Different Station Elevation

Figures 4.5 and 4.6 show the train's energy consumption with- and without regenerative braking. The graph consists of energy consumption results under high, medium, low, and no elevation scenarios. The energy consumptions for the train without regenerative braking for the elevation of 0 m, 0.464 m, 3.713 m, and 18.217 m are 40.37 kWh, 40.75 kWh, 42.29 kWh, and 46.30 kWh, respectively. Besides, the energy consumptions for the train with regenerative braking for the elevation of 0 m, 0.464 m, 3.713 m, and 18.217 m are 19.50 kWh, 20.02 kWh, 21.53 kWh, and 30.55 kWh, respectively. Table 4.3 summarize the energy consumption taken during each test run in case 3.
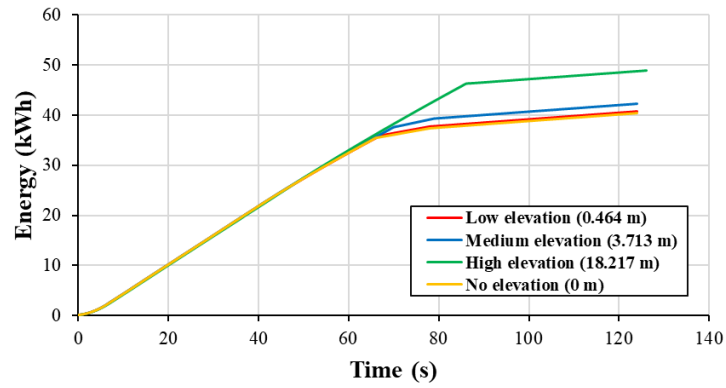
Figure 4.5: Power consumption of train at different elevations without regenerative braking system.
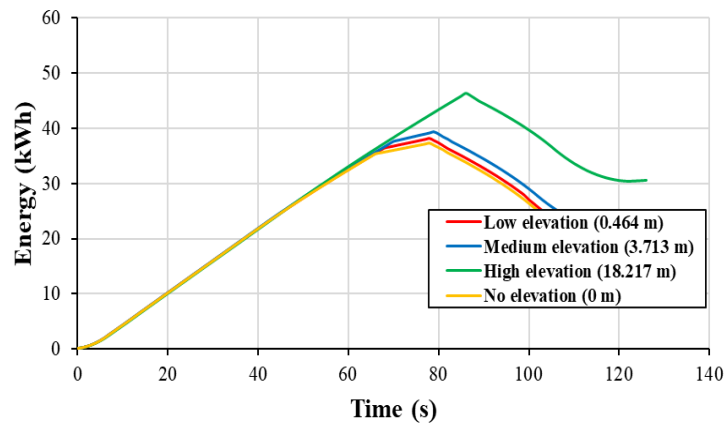
Figure 4.6: Power consumption of train at different elevations with regenerative braking system.

Table 4.3: Case 3 results.

Elevation (m)	Peak Energy Consumption with RBE (kWh)	Final Energy Consumption without RBE (kWh)	Final Energy Consumption with RBE (kWh)	Rate of Recuperation
0	37.34	40.37	19.50	51.70%
0.464	38.17	40.75	20.02	50.87%
3.713	39.33	42.29	21.53	49.09%
18.217	46.30	48.93	30.55	37.56%

The contribution of grade resistance increases the total tractive effort required for the train to reach the desired speed. Therefore, it causes the accumulated energy consumption to increase. When there is low elevation, the regenerative braking system can recuperate up to 50.87% of energy.

However, when the elevation is 18.2 m, the energy recuperate is only up to 37.56%, which shows that the increment in elevation can cause a decrease in the recuperation of regenerative braking energy.

4.6 Effect of Different Train Weight

Figure 4.7 and 4.8 shows the train's energy consumption with- and without regenerative braking when the weights of the train varied due to different loading scenarios. The graph consists of 152 tons, 218 tons, and 253 tons of energy consumption. The energy consumptions for the train without regenerative braking for the weight of 152 tons, 218 tons, and 253 tons are 30.68 kWh, 40.37 kWh, and 45.19 kWh, respectively. Besides, the energy consumptions for the train with regenerative braking for the weight of 152 tons, 218 tons, and 253 tons are 16.06 kWh, 19.50 kWh, and 20.96 kWh, respectively. Table 4.4 summarize the energy consumption taken during each test run in case 4.
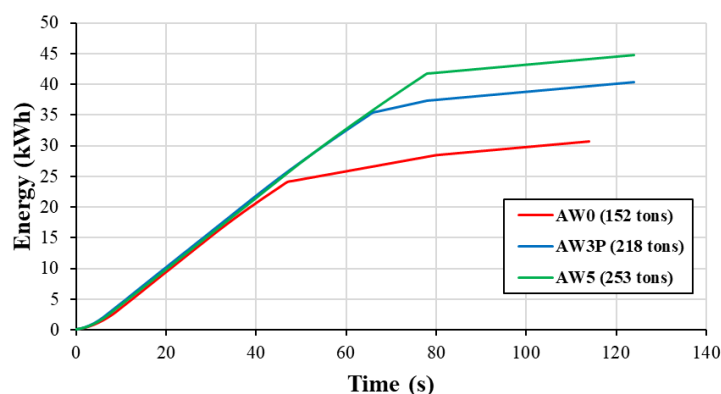
Figure 4.7: Power consumption of train at different train weights without regenerative braking system.
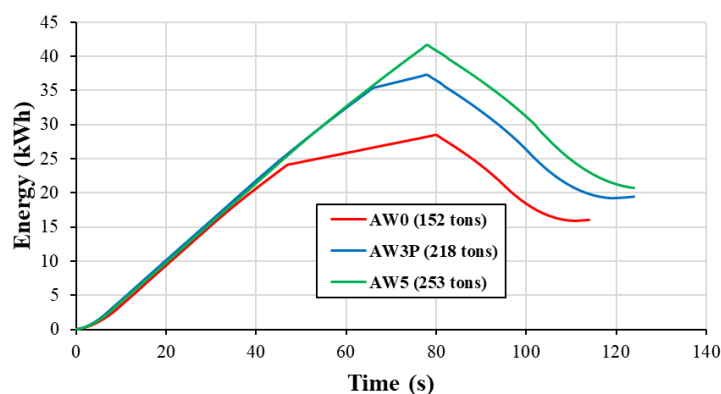
Figure 4.8: Power consumption of train at different train weights with regenerative braking system.

Table 4.4: Case 4 results.

Weight (ton)	Peak Energy Consumption with RBE (kWh)	Final Energy Consumption without RBE (kWh)	Final Energy Consumption with RBE (kWh)	Rate of Recuperation
152	28.45	30.68	16.06	47.65%
218	37.34	40.37	19.50	51.70%
253	41.71	45.19	20.96	53.62%

The test results show that by adding the weight from 152 tons to 253 tons, the increase in the total accumulated energy consumption can be up to 32% when no regenerative braking is applied and 23.4% when there is a regenerative braking system. The total energy recuperated when the train is at AW0, AW3P, and AW5 is 47.67%, 51.7%, and 53.62%, respectively. Therefore, it indicates that energy recuperation in the regenerative braking system increases when more weight is added to the rolling stocks.

4.7   Comparison between worst-case and optimum case

The model will be reconstructed into two different scenarios in this section. The initial state parameters will be set to the worst-case scenario for the first condition, including parameters with the lowest rate of regenerative braking energy recovery among the four scenarios. The parameters for the second scenario will be the highest rate of regenerative braking energy recovery from the four cases. Tables 4.5 and 4.6 show the parameters for the two studies.

Table 4.5: Parameters of worst-case.

System Description	Settings
Northbound distance (m)	2231
Southbound distance (m)	2224
Maximum acceleration / deceleration (m/s^2)	1
Dwell time (s)	40
Headway time (s)	109
Train's weight (tons)	152

Maximum Speed limit (km/h)	60
Station elevation (m)	18.217

Table 4.6: Parameters of optimum scenario.

System Description	Settings
Northbound distance (m)	900
Southbound distance (m)	900
Maximum acceleration / deceleration (m/s^2)	1
Dwell time (s)	40
Headway time (s)	109
Train's weight (tons)	253
Maximum Speed limit (km/h)	110
Station elevation (m)	0

After conducting the test with the two best and worst cases, the results are shown in Figures 4.9 and 4.10. The energy consumption for the worst scenario is having energy consumption of 28.02 kWh and 23.07 kWh of energy consumption with regenerative braking applied. In contrast, the energy consumption for the optimum scenario has an energy consumption of 24.94 kWh and 9.52 kWh of energy consumption with regenerative braking applied.
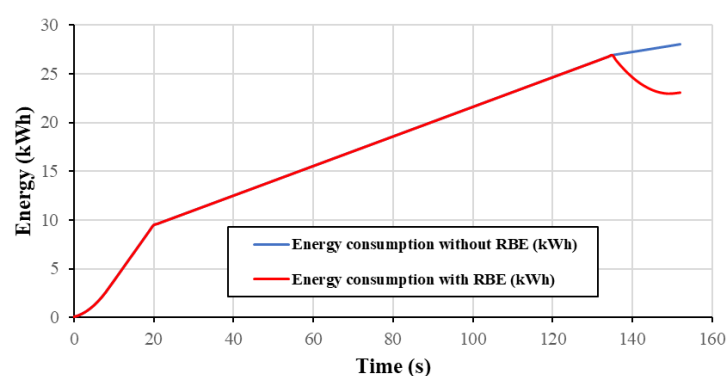
Figure 4.9: Power consumption curve with and without regenerative braking at worst-case scenario.
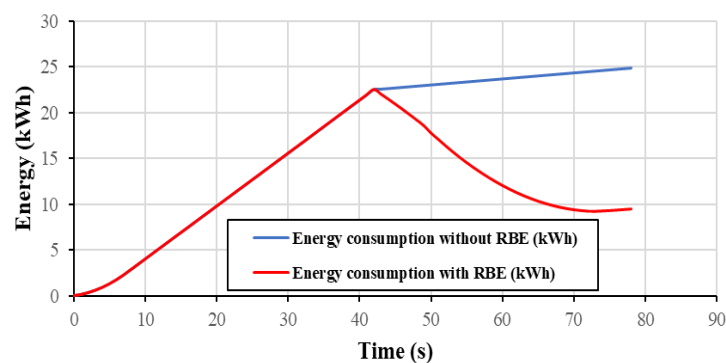
Figure 4.10: Power consumption curve with and without regenerative braking at optimum scenario.

Table 4.7: Comparison between worst-case and optimum case results.

Model Type	Peak Energy Consumption with RBE (kWh)	Final Energy Consumption without RBE (kWh)	Final Energy Consumption with RBE (kWh)	Rate of Recuperation
Worst Case	26.91	28.02	23.07	17.67%
Optimum Case	22.57	24.94	9.52	61.83%

According to Table 4.7, the worst-case scenario has just 17.67% energy recovery, while the optimal solution has 61.83% energy recovery. The difference in recovery rates between the worst- and best-case scenarios is 44.16%. As a result, maintaining the optimum scenario of low track lengths, high-speed limit, lowest elevation, and greatest weight can considerably increase the overall effectiveness of the regenerative braking system.

4.8 Summary

This chapter includes the findings from four research studies on the effects of stations distance, track speed limit, track elevation, and train weight under different loading conditions on the effectiveness of regenerative braking systems.

Based on the results, it is feasible to deduce that to optimize the regenerative braking system, the station distance should be kept as short as possible and allow for a higher speed limit during travel. Furthermore, for the

system to be more efficient, the elevation should be as low as possible, and the weight should be higher.

The comparisons between the worst case and the best scenario are also being investigated and discussed. The difference in efficiency between the best and worst cases can be as much as 44.16%.

CHAPTER 5

CONCLUSIONS AND RECOMMENDATIONS

5.1   Conclusions

This project investigates the impact of station distance, the track speed limit, the elevation of the train station, and the train's weight on the recuperation of energy in the railway electrification system.

For the investigation, a railway model based on Malaysia's MRT Line 2 was modeled in ETAP-eTraX. Two different models consisting of worst-case and optimum parameters are modeled to indicate differences in recuperation rate and study the effectiveness of strategies developed to improve system efficiency.

In order to maximize the performance of the regenerative braking system, the station distance should be kept as short as possible, the track's speed limit should be as high as feasible, the elevation should also be kept as low as possible, and the weight should be increased.

The simulation findings reveal that if the ideal situation of an optimal track length of 0.9 km is maintained, the regenerative braking system's maximum efficiency can reach 60.10%. Maintaining the most significant operational speed restrictions of 100 km/h, the lowest elevation, and the highest potential weight of the train, which is 253 tonnes with maximum passengers on board, the regenerative braking system's energy recovery efficiency can be up to 51.70%. When the worst-case scenario system is simulated, the energy recuperation is 17.67%. In contrast, the system with the optimum scenario has an energy recuperation of 61.83%. The results show that the systems have 44.16% difference in the recuperation of energy. A real-world measurement based on the Interface Test Procedure at MRT Line 2 is also being investigated, and the results are identical to the outcome of simulation results.

A conference paper entitled "An Investigation on Recuperation of Regenerative Braking Energy in DC Railway Electrification System" has

been presented and published in the IEEE Xplore under "The 2022 IEEE International Conference in Power Engineering Applications (ICPEA 2022)".

5.2 Recommendations for future work

An energy storage system can be utilized to stabilize voltage in short-term grid fluctuations, which can help solve power quality issues caused by poor voltage regulation. Voltage sags can cause short-term issues and disruptions, but frequent voltage excursions can shorten equipment life. This research can be used to reference future energy storage sizing and siting studies. Electrical information, such as peak voltage contributed by the generating system, may require installing an energy storage system or an inverter system. Many aspects must be considered when analyzing the effectiveness of energy storage for obtaining a more significant share of regenerative braking energy, and this study may serve as a reference.

REFERENCES

Bae, C.H., Jang, D.U., Kim, Y.G., Chang, S.K. and Mok, J.K., 2007. Calculation of regenerative energy in DC 1500V electric railway substations. In: *7th Internatonal Conference on Power Electronics, ICPE'07*. IEEE Computer Society.pp.801–805. https://doi.org/10.1109/ICPE.2007.4692497.

Dong, H., Ye, M., Jingang, G., Haoxuan, D., Sheng, W., Chao, T.U. and Min, Y.E., 2017. *Research of the Influence of Braking Conditions on Regenerative Braking Energy Recovery for Electric Vehicles International Symposium on Electric Vehicles Research of the Influence of Braking Conditions on Regenerative Braking Energy Recovery for Electric Vehicles*. [online] Available at: <https://www.researchgate.net/publication/327238167>.

Du, G., Zhang, D., Li, G., Wang, C. and Liu, J., 2016. Evaluation of Rail Potential Based on Power Distribution in DC Traction Power Systems. *Energies*, 9(9), p.729. https://doi.org/10.3390/en9090729.

Fazel, S.S., Firouzian, S. and Shandiz, B.K., 2014. *Energy-Efficient Emplacement of Reversible DC Traction Power Substations in Urban Rail Transport through Regenerative Energy Recovery*. *International Journal of Railway Research*.

Gao, Z., Lu, Q., Wang, C., Fu, J. and He, B., 2019. Energy-storage-based smart electrical infrastructure and regenerative braking energy management in AC-Fed railways with neutral zones. *Energies*, 12(21). https://doi.org/10.3390/en12214053.

González-Gil, A., Palacin, R. and Batty, P., 2013. *Sustainable urban rail systems: Strategies and technologies for optimal management of regenerative braking energy*. *Energy Conversion and Management*, https://doi.org/10.1016/j.enconman.2013.06.039.

Grassie, S.L. and Elkins, J.A., 2005. Tractive effort, curving and surface damage of rails: Part 1. Forces exerted on the rails. In: *Wear*. pp.1235–1244. https://doi.org/10.1016/j.wear.2004.03.064.

Günay, M., Korkmaz, M.E. and Özmen, R., 2020a. An investigation on braking systems used in railway vehicles. *Engineering Science and Technology, an International Journal*, 23(2), pp.421–431. https://doi.org/10.1016/j.jestch.2020.01.009.

Günay, M., Korkmaz, M.E. and Özmen, R., 2020b. An investigation on braking systems used in railway vehicles. *Engineering Science and Technology, an International Journal*, 23(2), pp.421–431. https://doi.org/10.1016/j.jestch.2020.01.009.

Khodaparastan, M., Mohamed, A.A. and Brandauer, W., 2019a. Recuperation of regenerative braking energy in electric rail transit systems. *IEEE Transactions on Intelligent Transportation Systems*, 20(8), pp.2831–2847. https://doi.org/10.1109/TITS.2018.2886809.

Khodaparastan, M., Mohamed, A.A. and Brandauer, W., 2019b. Recuperation of regenerative braking energy in electric rail transit systems. *IEEE Transactions on Intelligent Transportation Systems*, 20(8), pp.2831–2847. https://doi.org/10.1109/TITS.2018.2886809.

Lu, S., Weston, P., Hillmansen, S., Gooi, H.B. and Roberts, C., 2014. Increasing the regenerative braking energy for railway vehicles. *IEEE Transactions on Intelligent Transportation Systems*, 15(6), pp.2506–2515. https://doi.org/10.1109/TITS.2014.2319233.

Mayrink, S., Oliveira, J.G., Dias, B.H., Oliveira, L.W., Ochoa, J.S. and Rosseti, G.S., 2020. Regenerative braking for energy recovering in diesel-electric freight trains: A technical and economic evaluation. *Energies*, 13(4). https://doi.org/10.3390/en13040963.

Polach, O., 2001. *Influence of Locomotive Tractive Effort on the Forces Between Wheel and Rail. Vehicle System Dynamics Supplement*.

Popescu, M. and Bitoleanu, A., 2019. A review of the energy efficiency improvement in DC railway systems. *Energies*, 12(6). https://doi.org/10.3390/en12061092.

Sang Hoo, D., Yun Chong, K., Wang, L., Huat Chua, K., Seng Lim, Y., Cheun Hau, L. and Rong Chua, X., n.d. *An Investigation on Recuperation of Regenerative Braking Energy in DC Railway Electrification System*.

Hosseinipour, S. and Zolghadri, R., 2019. Effectiveness and Optimal Placement of Bidirectional Substations for Regenerative Braking Energy Recovery in Electrical Network of Metro System. *International Journal of Railway Research*, 6(2), pp.43-52.

Straub, L. and Jennison Knorr-Bremse, P., n.d. *State-of-the-art in commercial vehicle pneumatic disc brakes*.

Tian, Z., Zhao, N., Hillmansen, S., Roberts, C., Dowens, T. and Kerr, C., 2019. SmartDrive: Traction Energy Optimization and Applications in Rail Systems. *IEEE Transactions on Intelligent Transportation Systems*, 20(7), pp.2764–2773. https://doi.org/10.1109/TITS.2019.2897279.

Tian, Z., Zhao, N., Hillmansen, S., Su, S. and Wen, C., 2020. Traction power substation load analysis with various train operating styles and substation fault modes. *Energies*, 13(11). https://doi.org/10.3390/en13112788.

Wang, B., Yang, Z., Lin, F. and Zhao, W., 2014. An improved genetic algorithm for optimal stationary energy storage system locating and sizing. *Energies*, 7(10), pp.6434–6458. https://doi.org/10.3390/en7106434.

Wu, C., Lu, S., Xue, F., Jiang, L. and Chen, M., 2020. Optimal Sizing of Onboard Energy Storage Devices for Electrified Railway Systems. *IEEE Transactions on Transportation Electrification*, 6(3), pp.1301–1311. https://doi.org/10.1109/TTE.2020.2996362.

Xia, H., Chen, H., Yang, Z., Lin, F. and Wang, B., 2015. Optimal energy management, location and size for stationary energy storage system in a metro line based on genetic algorithm. *Energies*, 8(10), pp.11618–11640. https://doi.org/10.3390/en81011618.